

Review

Recent Innovative Progress of Metal Oxide Quantum-Dot-Integrated g-C₃N₄ (0D-2D) Synergistic Nanocomposites for Photocatalytic Applications

Tejaswi Tanaji Salunkhe ^{1,†}, Thirumala Rao Gurugubelli ^{2,†}, Bathula Babu ^{3,*} and Kisoo Yoo ^{3,*}

¹ Department of Chemical and Biological Engineering, Gachon University, Seongnam-si 13120, Republic of Korea; tejaswisalunkhe235@gmail.com

² Department of Physics, School of Sciences, SR University, Warangal 506 371, India; thirumala.phy@gmail.com

³ School of Mechanical Engineering, Yeungnam University, Gyeongsan 38541, Republic of Korea

* Correspondence: babuphysicist@ynu.ac.kr (B.B.); kisoo.yoo@yu.ac.kr (K.Y.)

† These authors contributed equally to this work.

Abstract: Modern industrialization has unleashed unprecedented environmental challenges, primarily in the form of pollution. In response to these pressing issues, the quest for innovative and sustainable solutions has intensified. Photocatalysis, with its unique capabilities, has emerged as a potent technology to combat the adverse effects of industrialization on the environment. This review highlights recent advances in harnessing photocatalysis to address environmental pollution. Photocatalysis offers a multifaceted approach, utilizing solar energy for catalytic reactions and enabling efficient pollutant removal. Quantum dots and graphitic carbon nitride (g-C₃N₄) are essential elements in this science. In contrast to quantum dots, which have enormous potential due to their size-dependent bandgap tunability and effective charge carrier production, g-C₃N₄ has properties like chemical stability and a configurable bandgap that make it a versatile material for photocatalysis. In this review, we explore recent achievements in integrating metal oxide quantum dots with g-C₃N₄, forming nanocomposites with superior photocatalytic activity. These nanocomposites exhibit extended light absorption ranges and enhanced charge separation efficiency, positioning them at the forefront of diverse photocatalytic applications. In conclusion, this comprehensive review underscores the critical role of photocatalysis as a potent tool to counteract the adverse environmental effects of modern industrialization. By emphasizing recent advancements in g-C₃N₄ and quantum dots and highlighting the advantages of metal oxide quantum dots decorated/integrated with g-C₃N₄ nanocomposites, this work contributes to the evolving landscape of sustainable solutions for environmental remediation and pollution control. These innovations hold promise for a cleaner and more sustainable future.



Citation: Salunkhe, T.T.; Gurugubelli, T.R.; Babu, B.; Yoo, K. Recent Innovative Progress of Metal Oxide Quantum-Dot-Integrated g-C₃N₄ (0D-2D) Synergistic Nanocomposites for Photocatalytic Applications. *Catalysts* **2023**, *13*, 1414. <https://doi.org/10.3390/catal13111414>

Academic Editors: Weilong Shi, Feng Guo, Xue Lin and Yuanzhi Hong

Received: 6 October 2023

Revised: 29 October 2023

Accepted: 1 November 2023

Published: 3 November 2023



Copyright: © 2023 by the authors. Licensee MDPI, Basel, Switzerland. This article is an open access article distributed under the terms and conditions of the Creative Commons Attribution (CC BY) license (<https://creativecommons.org/licenses/by/4.0/>).

1. Introduction

The ongoing march of progress, for eons, has been marked by humanity's relentless pursuit of industrialization. From the spinning jenny to the state-of-the-art factories dotting our landscapes, industrial processes have been the harbingers of prosperity, growth, and the advancement of our species [1]. Yet, this coin possesses a tarnished flip side. Our industrial accomplishments, while monumental, have brought with them undeniable environmental degradation. However, with its plethora of benefits, industrialization inadvertently ushered in a myriad of ecological challenges. Rapid urbanization and unchecked manufacturing processes spawned large-scale environmental pollution [2,3]. As industries mushroomed, so did the emissions, leading to the degradation of both air and water quality, affecting the very tenets of human health and environmental sustainability [4,5]. Among the myriad solutions that have been tabled to combat environmental degradation, one that stands

out for its potential and innovation is photocatalysis [6]. Rooted in the confluence of physics and chemistry, photocatalysis offers an avenue where pollutants are degraded under the influence of light [7]. This process is not only environment-friendly but also sustainable. The advantages of photocatalysis are manifold. Aside from its ability to degrade organic pollutants, it exhibits the potential to harness solar energy efficiently, making it an eco-friendly solution to some of the pressing challenges of our times [8].

Historically, the world of photocatalysis has witnessed the introduction and application of numerous catalysts, each bringing its own set of benefits and challenges. From the pioneering work on TiO_2 to the utilization of complex organic polymers, the field has never ceased to evolve [9,10]. Among these myriad materials, the realm of 2D and 3D materials has garnered significant interest [11,12]. Their unique morphologies, structural attributes, and ease of manipulation have made them frontrunners in the race to find the most efficient photocatalyst. In recent years, a material that has captured the imagination of researchers and scientists alike is graphitic carbon nitride, or $\text{g-C}_3\text{N}_4$ [13]. This two-dimensional material, with its layered structure reminiscent of graphene, has shown exceptional promise as a photocatalyst. The journey of $\text{g-C}_3\text{N}_4$ in the photocatalytic domain has been both evolutionary and revolutionary. Various precursors, ranging from urea to dicyandiamide, have been utilized in its synthesis, leading to variations in its properties and, consequently, its photocatalytic efficiency [14]. The synthesis of $\text{g-C}_3\text{N}_4$ is as intriguing as its properties. Various precursors, including melamine, dicyandiamide, and others, have been deployed to extract this material, with each method yielding slightly varied material properties, thereby influencing its overall photocatalytic performance [15].

Yet, even the most promising of materials present challenges. Issues with $\text{g-C}_3\text{N}_4$ include quick photogenerated electron–hole pair recombination, a narrow light absorption spectrum, and certain stability concerns, which have the potential to modestly shade the material's otherwise brilliant prospects. An innovative approach to overcoming these challenges is the hybridization of $\text{g-C}_3\text{N}_4$ with other materials, especially quantum dots, culminating in the creation of superior nanocomposites [16]. Quantum dots, particularly metal oxide quantum dots, have properties—such as size-tunable band gaps and a high surface-to-volume ratio—that are extraordinarily beneficial for photocatalysis. Their amalgamation with $\text{g-C}_3\text{N}_4$ brings forth synergistic effects, where the strengths of one complement the weaknesses of the other [17]. To combat $\text{g-C}_3\text{N}_4$'s limitations and further enhance its capabilities, researchers looked towards nanotechnology, specifically quantum dots. These nanosized semiconducting particles, notable for their quantum mechanical properties, brought several benefits [18]. Their size-dependent tunable band gaps, high surface reactivity, and ability to be easily integrated with other materials made them ideal partners for $\text{g-C}_3\text{N}_4$ [19]. Several quantum dots such as metal oxides, metal sulfides, carbon quantum dots, graphene quantum dots, etc., are integrated with $\text{g-C}_3\text{N}_4$ for superior photocatalytic performance [20–23].

Quantum size effects become prominent when the size of the semiconductor particles is reduced to the nanometer scale, approaching the exciton Bohr radius, resulting in quantum confinement. This phenomenon significantly alters the materials' electronic and optical properties, thereby influencing their photocatalytic behavior. For instance, as the particle size of these metal oxides decreases to the quantum scale, the bandgap can broaden due to the increased energy difference between the valence and conduction bands. This bandgap modification enhances light absorption efficiency and, subsequently, the photocatalytic performance under visible light, a feature not often observed in bulk counterparts. Specifically, in the realm of photocatalysis, nanosized TiO_2 and ZnO have demonstrated improved charge carrier generation due to their quantum-dot-like behavior. For instance, studies have shown that TiO_2 nanoparticles, with sizes reduced to the quantum realm (below 10 nm), exhibit a shift in their optical absorption toward the visible region, a direct consequence of the quantum size effect. Similarly, ZnO quantum dots (QDs) have been observed to display a higher photocatalytic activity compared to their bulk equivalents due

to their enlarged bandgap and more efficient charge separation, critical for processes like degradation of pollutants.

Within the quantum dot realm, metal oxide (TiO_2 , SnO_2 , CuO , ZnO) and metal sulfide (CdS , SnS_2 , MoS_2) quantum dots garnered significant attention [24–26]. Their inherent stability, coupled with favorable electronic properties, made them especially suited for photocatalytic applications [18,27,28]. Intense study has been conducted on the combination of $\text{g-C}_3\text{N}_4$ with quantum dots, also known as 2D-0D nanocomposites [20]. Significant milestones have been achieved, demonstrating enhanced photocatalytic activities, stability, and a broader range of light absorption [29]. This narrative, rich in scientific endeavors, merits a thorough review. It is imperative to collate, analyze, and critique the vast body of work that exists on this subject. For researchers delving deeper into this domain, there exists a myriad of opportunities [30]. The optimization of synthesis methods, exploring new combinations of quantum dots, and tuning the interfaces of these nanocomposites are just a few of the avenues that hold promise [31]. As this exciting chapter in photocatalysis continues to unfold, it remains a beacon of hope for a cleaner, more sustainable future. While this review intends to offer a comprehensive overview, it also serves as a clarion call to researchers worldwide. The field of $\text{g-C}_3\text{N}_4$ and quantum dot nanocomposites, though richly explored, is brimming with possibilities. Fresh perspectives, interdisciplinary collaborations, and novel methodologies can unearth nuances previously overlooked.

Impact of particle size on charge separation and catalytic kinetics:

Quantum Confinement Effect: as particle size reduces to the nanoscale, approaching the exciton Bohr radius, quantum confinement becomes prominent. This phenomenon significantly impacts the electronic properties of semiconductors, including the bandgap's widening. For photocatalysts, this can enhance absorption in the visible light range, crucial for solar-driven applications.

Increased Surface Area: smaller particles imply a larger surface area relative to volume, increasing the number of active sites available for reactions. This also facilitates the separation of charge carriers, as electrons and holes have shorter distances to travel to reach the surface, reducing recombination rates and enhancing photocatalytic efficiency.

Enhanced Charge Carrier Dynamics: the high surface-to-volume ratio at the nanoscale influences the redox potential of the material surface, creating more favorable conditions for charge transfer to the reactants, further discouraging charge recombination.

Catalyst–Reactant Interaction: smaller particles allow for more intimate contact with reactants due to their increased surface area, enhancing interaction frequency and energy transfer efficacy, which are critical for reaction kinetics.

Diffusion and Reaction Rates: nanosized materials modify diffusion rates of reactants and products. The shortened diffusion paths in smaller particles accelerate reaction rates, making them more efficient catalysts.

Activation Energy: the quantum size effect can modify the activation energy required for certain reactions. Quantum dots, due to their discrete energy levels, can lower the activation energy barriers, thereby accelerating the reaction kinetics.

2. Synthesis Protocols of $\text{g-C}_3\text{N}_4$

$\text{g-C}_3\text{N}_4$, an emerging two-dimensional polymer, has captivated researchers' interest primarily due to its remarkable physicochemical properties, making it a potential candidate for various applications, including photocatalysis [13]. Its unique electronic structure, environmental compatibility, and abundant natural precursors make $\text{g-C}_3\text{N}_4$ an attractive and eco-friendly material. In this comprehensive review, we delve into the synthesis protocols, precursor variations, morphology alterations, and their corresponding implications on photocatalytic performance. The synthesis of $\text{g-C}_3\text{N}_4$ generally revolves around thermally induced polymerization of nitrogen-rich precursors. The following are notable synthesis routes: (a) Direct Thermal Polymerization—in this method, nitrogen-rich organic precursors like melamine or urea are directly heated to temperatures between 500 and 600 °C, leading to polymerization and subsequent formation of $\text{g-C}_3\text{N}_4$ [32]. (b) Solvent-assisted

Synthesis—by incorporating solvents, the crystallinity and porosity of $\text{g-C}_3\text{N}_4$ can be manipulated, enhancing its performance in specific applications. (c) Microwave-assisted Synthesis—this method harnesses the rapid heating capabilities of microwaves to achieve efficient and homogenous polymerization.

Several precursors for $\text{g-C}_3\text{N}_4$ synthesis, distinguished by their nitrogen content, can be employed for $\text{g-C}_3\text{N}_4$ synthesis: (a) Melamine—owing to its high nitrogen content, melamine is a widely preferred precursor. It affords good crystallinity and relatively more uncondensed amino groups, beneficial for certain applications [33]. (b) Urea—a more economical alternative, urea can be directly polymerized to yield $\text{g-C}_3\text{N}_4$. However, urea-derived $\text{g-C}_3\text{N}_4$ often displays inferior crystallinity [32]. (c) Dicyandiamide—it serves as an intermediate between melamine and urea in terms of the nitrogen content and resulting material properties [34]. The morphological attributes of $\text{g-C}_3\text{N}_4$ are significantly dictated by the thermal treatment it undergoes (Figure 1). Two parameters, the duration and ramping rate of the heating process, play pivotal roles: (a) Temperature Duration—extended heating times can refine the crystalline structure but might lead to an over-condensed framework, reducing activity in certain applications [32]. (b) Ramping Rate—a rapid ramping rate can cause abrupt polymerization, potentially resulting in non-uniform morphology. Gradual heating, on the other hand, allows a more ordered structure to be formed.

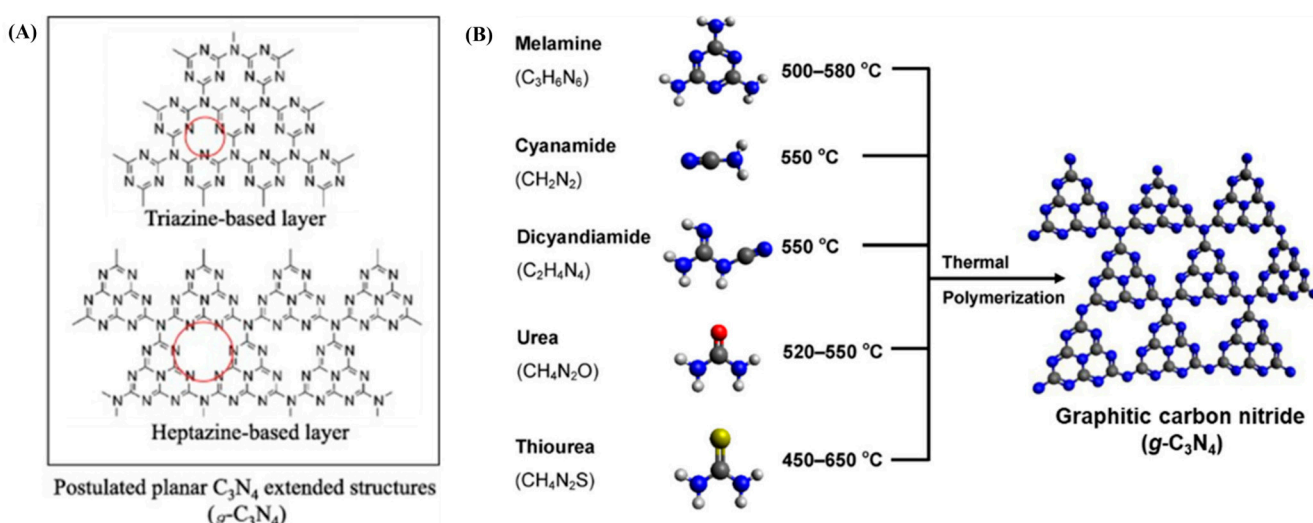


Figure 1. (A,B) Synthesis of $\text{g-C}_3\text{N}_4$ from different precursors and temperature conditions [35].

Over the years, researchers have reported a diverse array of $\text{g-C}_3\text{N}_4$ morphologies like nanosheets, nanorods, nanolayers, etc., due to their specific reasons [36]. Bulk $\text{g-C}_3\text{N}_4$ provides the primary structure obtained from direct thermal polymerization, characterized by its layered architecture. $\text{g-C}_3\text{N}_4$ nanosheets are thin, 2D planar structures that exhibit a higher surface area compared to the bulk counterpart. $\text{g-C}_3\text{N}_4$ nanorods are one-dimensional nanostructures offering directional pathways for charge transport. $\text{g-C}_3\text{N}_4$ nanolayers are ultrathin variants of nanosheets, further maximizing the surface area. $\text{g-C}_3\text{N}_4$ porous nanosheets introducing porosity can facilitate greater substance interaction and accessibility [37].

Several strategies exist to induce desired morphological changes in $\text{g-C}_3\text{N}_4$. (a) Exfoliation: mechanical or chemical means can be employed to delaminate bulk $\text{g-C}_3\text{N}_4$, producing nanosheets [38]. (b) Template Method: using sacrificial templates, $\text{g-C}_3\text{N}_4$ can be cast into specific morphologies, like rods or spheres, which are subsequently removed [39]. (c) Direct Synthesis: by manipulating synthesis conditions, such as precursor concentration or solvent choice, varied morphologies can be achieved [40]. The morphological modifications directly impact $\text{g-C}_3\text{N}_4$'s performance in photocatalysis. Enhanced surface area, improved light absorption, efficient charge separation, and facile substance accessibility are some of the benefits brought by morphology optimization. From its synthesis from diverse

precursors to the myriad morphologies it can adopt, g-C₃N₄ offers an exciting playground for materials scientists and engineers. As our understanding of its structure–performance relationship deepens, fine-tuned g-C₃N₄ materials, specifically designed for target applications, can be anticipated. By marrying the principles of green chemistry with advanced characterization and simulation techniques, the next chapter in the g-C₃N₄ saga is set to be even more promising.

Role of advanced spectroscopic techniques:

Researchers must know the importance of understanding the underlying mechanisms responsible for the high photocatalytic activity of g-C₃N₄-QD nanocomposites.

Absorption and Bandgap Analysis: enhanced absorption in the visible-light region is a key indicator of improved photocatalytic activity. When quantum dots (QDs) are integrated with g-C₃N₄, a noticeable shift in the absorption edge towards longer wavelengths can be observed. This suggests a reduced bandgap, allowing the composite to harness a greater portion of the solar spectrum. A reduced bandgap often leads to increased electron–hole pair generation, thus driving photocatalytic reactions more efficiently [26].

Photoluminescence (PL) Spectroscopy: PL studies offer invaluable insights into the recombination rates of photoinduced electron–hole pairs. For an effective photocatalyst, the suppression of this recombination is crucial. Post integration of QDs with g-C₃N₄, a significant quenching or decrease in the PL intensity can be observed, signifying reduced recombination rates. This reduced recombination, as evidenced by the PL studies, supports the notion of heightened photocatalytic performance of the composite [19].

X-ray Photoelectron Spectroscopy (XPS): XPS is instrumental in probing the surface electronic states of materials. Upon forming a heterojunction between g-C₃N₄ and QDs, shifts in the XPS peak positions can be noticed, indicating a change in the electronic environment and suggesting charge transfer between the constituents. The altered intensities can hint at the difference in elemental composition, showcasing the successful integration of QDs onto g-C₃N₄. Such charge transfer is paramount for separating the photogenerated electron–hole pairs, thereby enhancing the photocatalytic efficiency [21].

Other Spectroscopic Techniques: Electron Paramagnetic Resonance (EPR) can be employed to detect photoinduced radical species, directly supporting the photocatalytic activity of the material. Additionally, techniques like Fourier-transform infrared spectroscopy (FTIR) can offer insights into the surface functional groups, ensuring the stability and integrity of the composite during photocatalytic reactions [24].

3. Metal Oxide QD-g-C₃N₄ Nanocomposites

Advantages of quantum dots over nanoparticles:

Size and Quantum Confinement: the primary distinction lies in the size. Quantum dots are typically smaller than nanoparticles and are in the range of 1–10 nanometers (approximately 10–50 atoms in diameter). At this scale, quantum effects significantly influence the material's properties, leading to phenomena like quantum confinement in semiconductor QDs, which is not observed in larger nanoparticles. This results in unique optical, electronic, and catalytic properties for QDs.

Optical Properties: due to quantum confinement, QDs exhibit size-dependent tunable photoluminescence, allowing them to absorb and emit light over a wide spectrum. This property is crucial for various applications, including photocatalysis, and is not prominently observed in larger nanoparticles.

Surface Properties: the high surface-to-volume ratio of QDs leads to a significant proportion of atoms being at the surface, which profoundly impacts their chemical reactivity and catalytic activity. While nanoparticles also have a high surface-to-volume ratio, the quantum effects in QDs enhance these surface-related properties.

Energy Band Structures: the discrete energy levels in QDs, a consequence of quantum confinement, differ substantially from the continuous band structure of bulk materials or larger nanoparticles. This affects their interaction with light, charge carrier generation, and transfer—critical factors in photocatalytic processes.

3.1. Wide-Bandgap Metal Oxide QD-g-C₃N₄ Nanocomposites

In recent half-decade research, TiO₂ quantum dots (QDs) have solidified their position as stalwarts in the realm of nanotechnology, largely attributed to their exceptional photocatalytic proficiencies [41]. These quantum entities hold immense promise in efficiently absorbing solar energy, paving the way for their integration into an array of environmental and energy-focused applications. Properties intrinsic to TiO₂ QDs set them apart in the vast quantum landscape. The quantum confinement effect empowers them with a modifiable bandgap, a boon for diversifying photocatalytic ventures. Their magnified surface-to-volume ratio augments their inherent reactivity, and their commendable photostability ensures longevity in demanding applications [42]. As for their real-world implications, these QDs shine in water purification, adeptly obliterating organic contaminants. Their prowess extends to hydrogen production, where they serve as linchpins in photoelectrochemical water splitting. Furthermore, their capabilities in air purification, specifically in annihilating noxious air pollutants, have been documented. In essence, the ongoing research narrative accentuates the transformative potential of TiO₂ QDs, suggesting a luminous path ahead in environmental rejuvenation and sustainable energy paradigms. According to Wang et al., creating a p-TiO₂ QDs@g-C₃N₄ p-n junction results in better photocatalytic performance than using pure g-C₃N₄. The improved performance is a result of the p-n heterojunction, strong interface interaction, and quantum-size impact [43]. Wang (2021) synthesized an F-doped TiO₂ quantum dot/g-C₃N₄ nanosheet Z-scheme photocatalyst through chemical bonding, resulting in improved oxidizability, reducibility, and interfacial charge transfer ability [44]. Lee (2023) created a 0D/2D heterojunction nanocomposite with TiO₂ quantum dots anchored on g-C₃N₄ nanosheets (Figure 2) that demonstrated accelerated solar-driven photocatalysis [45]. The integration of anatase/rutile homojunction quantum dots onto g-C₃N₄ nanosheets, which is intended to target the breakdown of antibiotics in saltwater matrices, was documented by Hu and colleagues. Their study delves into the combined mechanism of adsorption and photocatalysis, shedding light on its underlying intricacies. They further evaluated the ternary heterojunctions formed between anatase/rutile quantum dots (QDs) and g-C₃N₄, emphasizing their effectiveness in the removal of Oxytetracycline (OTC). Additionally, the research gauges the toxicity levels of the resultant intermediates detected post-process [24].

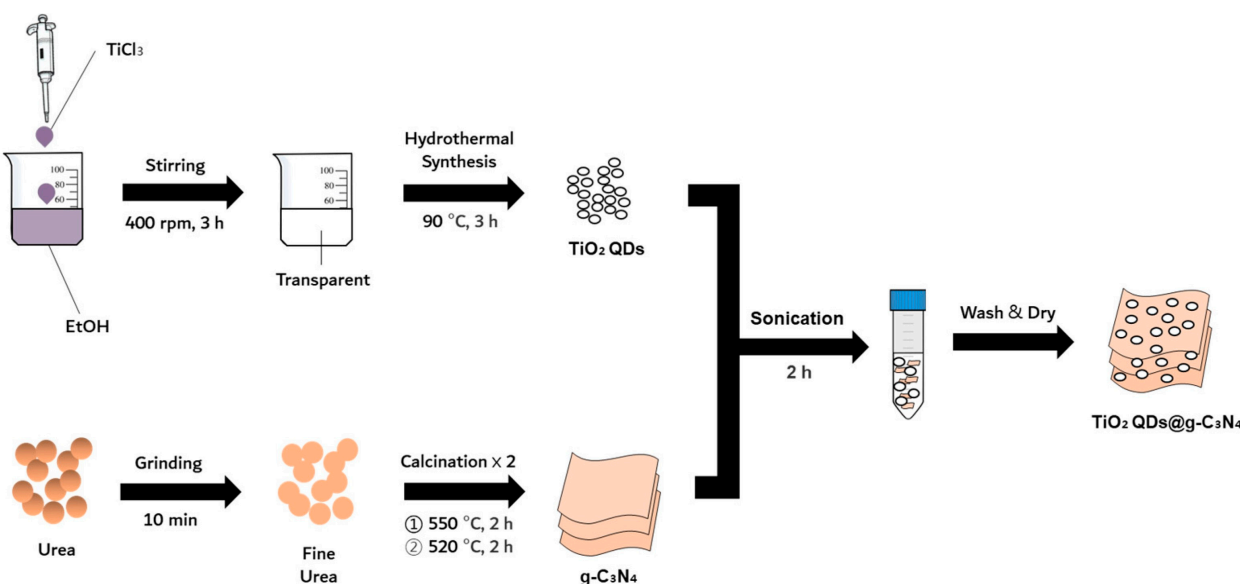


Figure 2. Synthetic process for fabricating TiO₂ QDs@g-C₃N₄ nanocomposite [45].

In recent years, the world of nanotechnology has seen an upswing in interest towards SnO₂ quantum dots (QDs), primarily owing to their potent capabilities in photocatalysis [46]. These quantum dots excel in efficiently harnessing light, thereby driving effective charge

separation and curbing recombination—traits indispensable for successful photocatalysis. Delving into their synthesis, several cutting-edge methods have emerged over the past half-decade. The hydrothermal method, which revolves around reacting tin salts in water under specific temperature and pressure conditions, remains a favored choice [47]. However, the sol-gel approach, where a precursor solution transitions from a gel-like consistency to the desired quantum dots upon drying and calcination, is also prevalent [46]. Not to be overshadowed, the microwave-assisted synthesis leverages the power of uniform and rapid microwave heating, often resulting in SnO_2 QDs of superior crystallinity in a fraction of the conventional synthesis time [48]. What truly sets SnO_2 QDs apart are their intrinsic properties. The quantum confinement effect grants researchers the liberty to tweak their bandgap, ensuring adaptability for a range of light-driven reactions. Their nanoscale stature bestows upon them a vast surface area, ideal for fostering enhanced reactant interactions. Furthermore, they stand out in the quantum dot family for their remarkable chemical and thermal stability. On the application front, these QDs have been instrumental in several arenas, from water splitting, where they play a role in converting water into hydrogen fuel using sunlight, to the degradation of persistent organic pollutants in water [49]. Another noteworthy application is their potential in reducing CO_2 , where they can transform atmospheric carbon dioxide into valuable fuels, presenting a promising avenue to combat escalating CO_2 levels [50]. Recent studies and trends hint that the true potential of SnO_2 QDs, especially when amalgamated with complementary materials, is yet to be fully unlocked, holding promises for advances in sustainable energy and environmental solutions.

SnO_2 quantum dots (QDs) with graphitic carbon nitride ($\text{g-C}_3\text{N}_4$) can improve photocatalytic activity. In 2018, Babu found that when exposed to sunlight, the mixture of SnO_2 QDs and $\text{g-C}_3\text{N}_4$ nanolayers displayed increased photocatalytic performance, effectively breaking down methyl orange. This increase in sunlight-driven photocatalytic activity is attributed to the cooperative interaction between the $\text{g-C}_3\text{N}_4$ nanolayers and SnO_2 quantum dots. These results highlight the potential of $\text{g-C}_3\text{N}_4$ nanolayers and SnO_2 QDs as powerful sunlight-responsive photocatalysts, particularly for the degradation of pollutants like methyl orange [27]. In 2019, Yousaf noted a marked increase in photocatalytic performance upon the embellishment of $\text{g-C}_3\text{N}_4$ with SnO_2 QDs, which led to the successful decomposition of Rhodamine B. The relative proportion of SnO_2 to $\text{g-C}_3\text{N}_4$ in these nanohybrids plays a pivotal role in determining their photocatalytic efficacy (Figure 3). Such findings highlight the potency of $\text{SnO}_2/\text{g-C}_3\text{N}_4$ nanocomposites, particularly in the domain of degrading contaminants like Rhodamine B (RhB) in solutions [51]. In 2017, Ji pioneered the synthesis of a composite photocatalyst combining SnO_2 with graphene-like $\text{g-C}_3\text{N}_4$. This composite exhibited superior visible-light-driven activities in degrading organic pollutants. Remarkably, its optimal photocatalytic efficiency under visible light exposure surpassed that of SnO_2 and $\text{g-C}_3\text{N}_4$ by almost 9 and 2.5 times, respectively [52]. The synergy between SnO_2 and graphene-like $\text{g-C}_3\text{N}_4$ is highlighted in this composite, which is represented as $\text{SnO}_2/\text{graphene-like g-C}_3\text{N}_4$, underlining its potential in photocatalytic processes. Its process in the degradation of Rhodamine B (RhB) with visible light in particular provides encouraging insights into its functional possibilities. All of these results point to the possibility that SnO_2 quantum dots and $\text{g-C}_3\text{N}_4$ work better together to accelerate photocatalytic breakdown of organic contaminants in water.

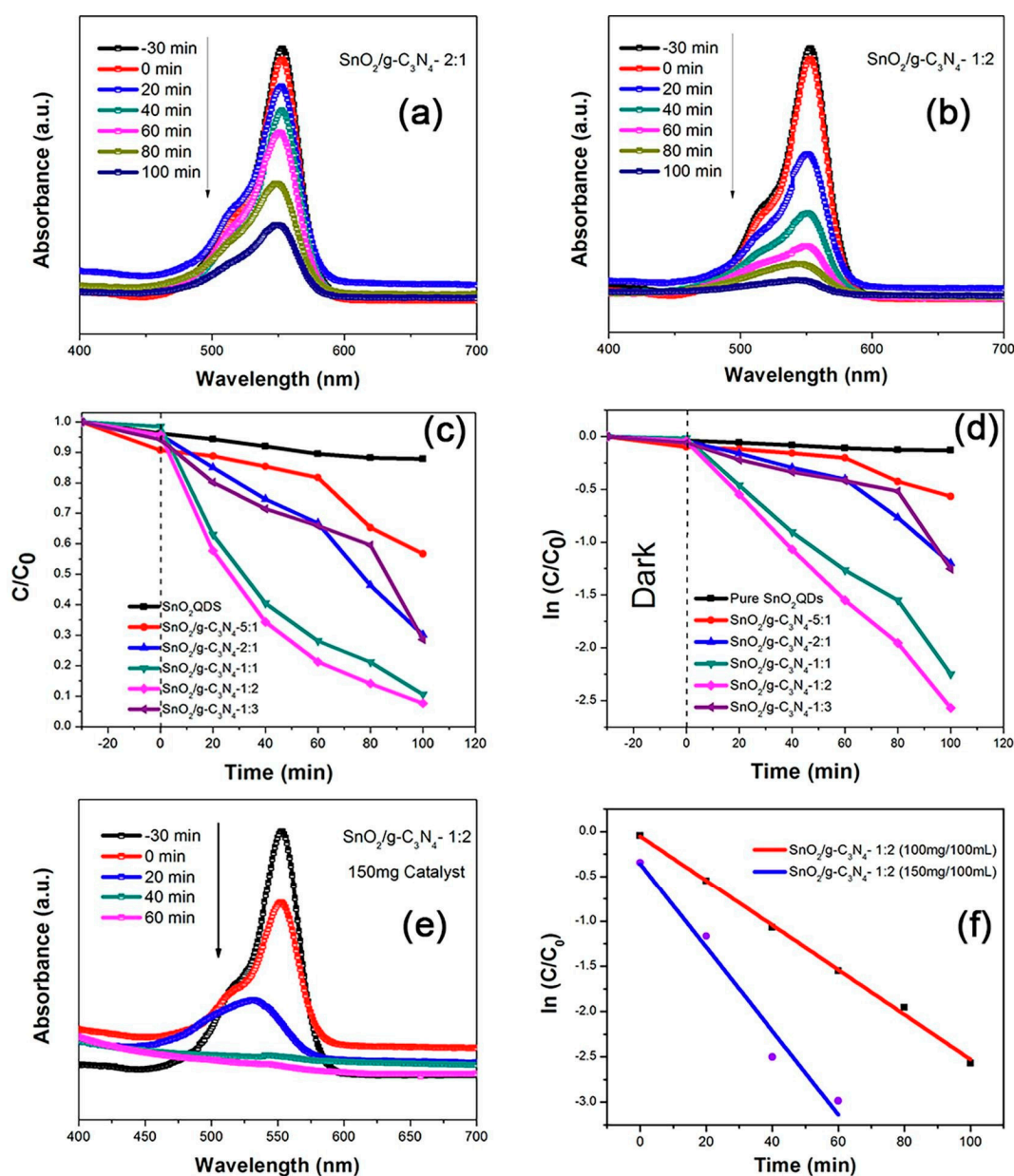


Figure 3. (a–f) Photocatalytic application of SnO_2 QD/ $\text{g-C}_3\text{N}_4$ nanocomposite [51].

Zinc oxide (ZnO) quantum dots have shown significant promise for photocatalytic applications, driven by their unique physicochemical properties. ZnO quantum dots exhibit enhanced photocatalytic efficiency owing to their high surface area and quantum confinement effects [53]. Their ability to generate reactive oxygen species upon light irradiation makes them potent catalysts for degrading organic pollutants. Researchers have delved into surface modifications to improve the photocatalytic performance of ZnO quantum dots [54]. Techniques like doping, coating, or hybridizing with other materials have been shown to enhance their stability and photocatalytic activity. The advent of black ZnO quantum dots has opened up the possibility of utilizing visible light, significantly broadening the spectrum of light that can be used for photocatalytic applications. Innovations in the design of heterostructures with ZnO quantum dots have shown promise in promoting charge separation, which is crucial for efficient photocatalysis. ZnO quantum dots have found real-world applications in water treatment, air purification, and energy conversion, embodying the translation of academic research to practical solutions [55]. Studies have showcased the robustness of ZnO quantum dots in diverse environmental conditions,

highlighting their potential for outdoor applications. The integration of ZnO quantum dots with other nanomaterials like graphitic carbon nitride has led to the creation of novel nanocomposites with superior photocatalytic properties [56]. Ren et al. created a composite by mixing graphitic carbon nitride ($\text{g-C}_3\text{N}_4$) and ZnO quantum dots (QDs) with the goal of enhancing the material's photocatalytic properties. It was impressive to see how well the composite degraded Rhodamine B when exposed to visible light. A 96.8% degradation rate of Rhodamine B was attained under visible light within a 40 min window, which was a startling achievement. This heightened photocatalytic efficacy is believed to emanate from the synergistic interplay between ZnO QDs, GO, and $\text{g-C}_3\text{N}_4$. The separation of photo-generated electron–hole pairs was accelerated with this combination [57]. In conclusion, the ZnO QD/GO/ $\text{g-C}_3\text{N}_4$ composite emerges as a potent contender for the remediation of organic pollutants in wastewater, presenting a workable solution for real-world wastewater treatment scenarios. This is due to its potent photocatalytic performance under visible light and its impressive durability. Investigating the visible-light-induced photocatalytic behavior of SnO_2 -ZnO quantum dots attached to $\text{g-C}_3\text{N}_4$ nanosheets was the goal of Vattikuti et al. The two main areas of concern were the degradation of contaminants and the creation of H_2 . They successfully anchored SnO_2 -ZnO quantum dots onto $\text{g-C}_3\text{N}_4$ nanosheets with their efforts. The resultant composite manifested heightened photocatalytic prowess when exposed to visible light, especially evident in its commendable degradation rates for contaminants like RhB and phenol. When the data were analyzed, it was discovered that the composite's RhB degradation rate was 3.5 times greater than that of pure $\text{g-C}_3\text{N}_4$. Similar to this, phenol's rate of degradation was 2.8 times more rapid than that of $\text{g-C}_3\text{N}_4$. Additionally, it was found that the composite's capacity to produce H_2 was astonishingly 4.6 times greater than that of pure $\text{g-C}_3\text{N}_4$. From these results, it is clear that the SnO_2 -ZnO quantum dots, when attached to $\text{g-C}_3\text{N}_4$ nanosheets, significantly improve photocatalytic activity when exposed to visible light. This composite not only excels at degrading pollutants but also evinces significant potential in H_2 production. Such attributes earmark it as a viable solution for tasks ranging from environmental purification to fostering sustainable energy methodologies [58].

3.2. Bi-Based QD- $\text{g-C}_3\text{N}_4$ Nanocomposites

Bismuth-based quantum dots (QDs) have emerged as a captivating class of nanostructured semiconductors, drawing substantial interest because of their unique electronic, optical, and photocatalytic characteristics. Their size-dependent bandgaps offer specific tunability for photocatalytic reactions. BiVO_4 QDs [59], for instance, display improved light absorption due to quantum confinement effects, and they are recognized for their proficiency in visible-light-driven water splitting and pollutant degradation (Figure 4). Bismuth oxide (Bi_2O_3) QDs exhibit enhanced optical attributes and charge transfer characteristics, positioning them as formidable catalysts for UV and visible light pollutant degradation [31,60]. Bi_2WO_6 QDs, with their increased electron–hole separation at the quantum level, stand out in degrading diverse organic pollutants under visible light [61]. While Bi_2O_4 QDs are relatively less explored, they have demonstrated potential with amplified light interaction at the nanoscale and offer efficient photocatalytic reactions. Lastly, Bi_2MoO_6 quantum dots, known for their extended photogenerated charge carrier lifetimes, are potential frontrunners for organic compound degradation and hydrogen evolution tasks [62]. In a nutshell, the nano-dimensionality of bismuth-based QDs accentuates their photocatalytic performance by amplifying light absorption, optimizing charge transfer, and minimizing recombination, making them versatile contenders for an array of photocatalytic applications. The scientists wanted to create a ternary heterostructure comprising C60, $\text{g-C}_3\text{N}_4$, and BiVO_4 quantum dots as a photocatalyst. This was carried out to increase the photocatalytic activity when exposed to visible light. Under visible light irradiation, the synthesized ternary heterostructure shown improved photocatalytic activity. Compared to binary heterostructures and pure $\text{g-C}_3\text{N}_4$, the ternary heterostructure showed a greater photocatalytic degradation rate of Rhodamine B (RhB) [59]. The higher charge separation

efficiency and expanded light absorption range were credited with the better photocatalytic performance. The potential mechanisms underlying the ternary heterostructure's improved photocatalytic activity were discussed by the researchers. They emphasized how C₆₀ and BiVO₄ quantum dots worked together to promote charge separation and lessen recombination. The enhanced photocatalytic efficiency of the ternary heterostructure was also attributed to a wider light absorption range. In comparison to other structures, the ternary heterostructure of BiVO₄ quantum dots/C₆₀/g-C₃N₄ was effectively constructed and showed higher photocatalytic activity. The study offers suggestions for creating effective photocatalysts for a variety of uses, including environmental cleanup.

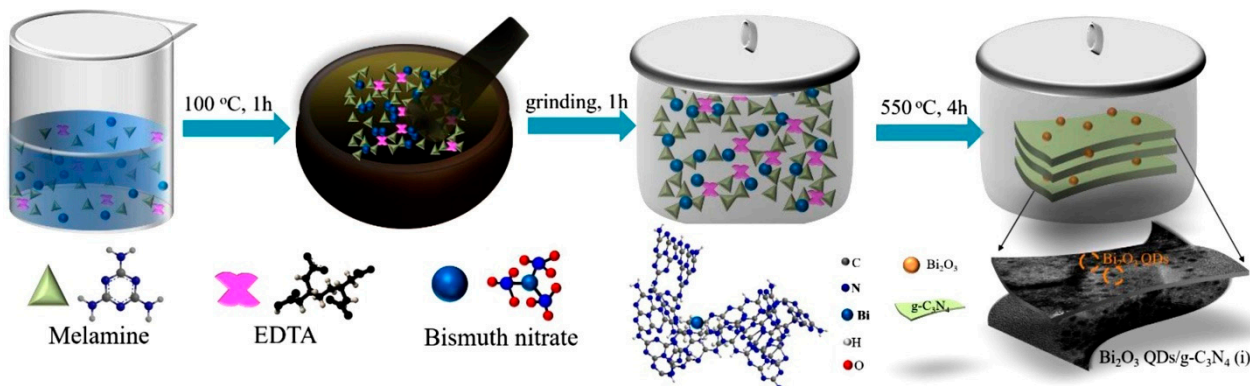


Figure 4. Schematic diagram of the synthesis process for Bi₂O₃ QD/g-C₃N₄ nanocomposite [60]. Copyright 2021, Elsevier.

Liang et al. looked at how well Bi₂O₃ QDs/g-C₃N₄ performed as a photocatalyst for both organic and inorganic contaminants. Tetracycline (TC) and Cr (VI) were chosen as representative environmental pollutants to assess the effectiveness of the samples' photocatalytic reduction and oxidation [60]. Under light illumination, the photocurrent density of the Bi₂O₃ QDs/g-C₃N₄ (ii) was noticeably higher than that of the g-C₃N₄, E-g-C₃N₄, and Bi₂O₃ QDs/g-C₃N₄, showing better charge transfer efficiency. Bi₂O₃ QDs/g-C₃N₄ had the shortest semicircular arc diameter, according to EIS Nyquist plots, indicating the lowest charge transfer resistance and quickest interfacial charge transport. Scavengers had an impact on the effectiveness of TC's degradation, proving that certain radicals were involved in the process. Byproducts of TC were produced using photocatalytic mineralization processes, with some intermediates demonstrating decreased toxicity after photocatalytic degradation. Bi₂O₃ QDs/g-C₃N₄ underwent photoinduction to improve the separation and transfer of photogenerated charges. As model environmental pollutants, TC and Cr (VI) were used to assess the photocatalytic performance. For Bi₂O₃ QDs/g-C₃N₄, the results showed increased charge transfer effectiveness and quicker interfacial charge transport. The research showed that Bi₂O₃ QDs/g-C₃N₄ had the potential to be an efficient photocatalyst for the oxidation of both organic and inorganic contaminants. Its better photocatalytic performance was aided by its improved charge transfer efficiency and decreased charge transfer resistance. The research offers a potential method for creating highly scattered metal oxides on 2D lamella semiconductors, expanding the photocatalyst's usefulness for removing a variety of environmental pollutants. Zeng et al. concentrated on the logical application of quantum dots (QDs) and graphitic carbon nitride (g-C₃N₄) semiconductors to increase their effectiveness as photocatalysts. The integration of g-C₃N₄ with QDs was intended to increase photogenerated electron transfer efficiency and produce significant photocatalytic activity. The researchers created brand-new Bi₂WO₆ QD/g-C₃N₄ nanocomposites with attapulgite (ATP) penetration [61]. The outcomes demonstrated that the ATP with a nanorod shape served as bridges to intercalate into the interlayers, thus enlarging the g-C₃N₄ inner space. With the use of an HPLC-MS system, the samples' photocatalytic degradation activities were examined. Using a specified formula, the degrading effectiveness of MBT in the solution was determined. The MBT solution was broken down while

being exposed to radiation to gauge the photocatalytic performance. We examined the rate of MBT degradation in several samples and investigated the photocatalytic degradation processes. The BCA5 sample exhibited favorable photoelectric characteristics, which indicated quick interfacial charge movement and low resistance for the production of charge carriers. As a potential strategy for future photocatalytic applications, the integration of g-C₃N₄ and QDs with the interpenetration of ATP led to improved photocatalytic performance. In order to create a 2D-0D g-C₃N₄/Bi₂WO₆-OV composite catalyst, Cheng et al. combined two-dimensional (2D) graphite carbon nitride (g-C₃N₄) nanosheets with oxygen-containing vacancy zero-dimensional (0D) Bi₂WO₆ (BWO-OV) quantum dots [31]. The goal was to improve the catalyst's catalytic activity, increase the formation of photogenerated carriers, and improve light absorption. Utilizing Bi₂WO₆ with oxygen vacancies, which improved light absorption while simultaneously increasing the production of photogenerated carriers, was the novel method. The vacancy structure of Bi₂WO₆ and the heterojunction's creation both contributed to the photogenerated carriers' longer longevity. The composite of CN/BWO-OV-10 displayed the maximum intensity, indicating a greater capacity for NO degradation. The outcomes of the trapping tests revealed that superoxide radicals, holes, and electrons all contribute significantly to the photocatalytic reaction. Furthermore, hydroxyl is recognized as a less potent active free radical. By eliminating NO, the photocatalytic effectiveness was evaluated. The efficiency peaked at 61.2% when BWO-OV was 10% by mass of the total amount of CN. The CN/BWO composite demonstrated the superiority of CN/BWO-OV-10 with a rise in efficiency of 3.2%, achieving a degradation efficiency of 58%. At room temperature, the composite g-C₃N₄/Bi₂WO₆-OV structure removed nitric oxide (NO) at a rapid rate despite its low concentration. The composite catalyst's efficiency was higher than that of g-C₃N₄ or BWO-OV and superior to that of g-C₃N₄/Bi₂WO₆ without oxygen vacancies. The best catalytic activity was demonstrated with the composite g-C₃N₄/Bi₂WO₆-OV-10, reaching up to 61.2%. The substance also demonstrated outstanding stability throughout several iterations of experimentation.

Ding and co. investigated Bi₂MoO₆ QDs/g-C₃N₄ with heterojunctions for their potential in the selective oxidation of aromatic alkanes into aldehydes under visible-light-driven catalysis [62]. The study offers fresh insights into the manufacturing of 0D/2D photocatalysts with heterojunctions for effective selective oxidation of C(sp³)-H bonds (Figure 5). It also presents a novel structure that improves the separation of charge carriers. Outstanding visible-light-driven catalytic performance was shown with the Bi₂MoO₆ QD/g-C₃N₄ heterojunction in the selective oxidation of aromatic alkanes into aldehydes. The heterojunction's special structure, which facilitates the effective separation of charge carriers, is said to be responsible for the increased photocatalytic activity. Superior photocatalytic activity was demonstrated with the heterojunction of Bi₂MoO₆ QDs/g-C₃N₄, particularly in the selective oxidation of aromatic alkanes. The distinctive structure that enables greater charge carrier separation is responsible for this performance. Under visible light, the Bi₂MoO₆ QD/g-C₃N₄ heterojunction exhibits outstanding photocatalytic activity in the selective oxidation of aromatic alkanes to aldehydes. The distinctive structure, which improves charge carrier separation, is credited with the efficiency. The potential of 0D/2D photocatalysts with heterojunctions for the selective oxidation of C(sp³)-H bonds is crucial information provided in this study.

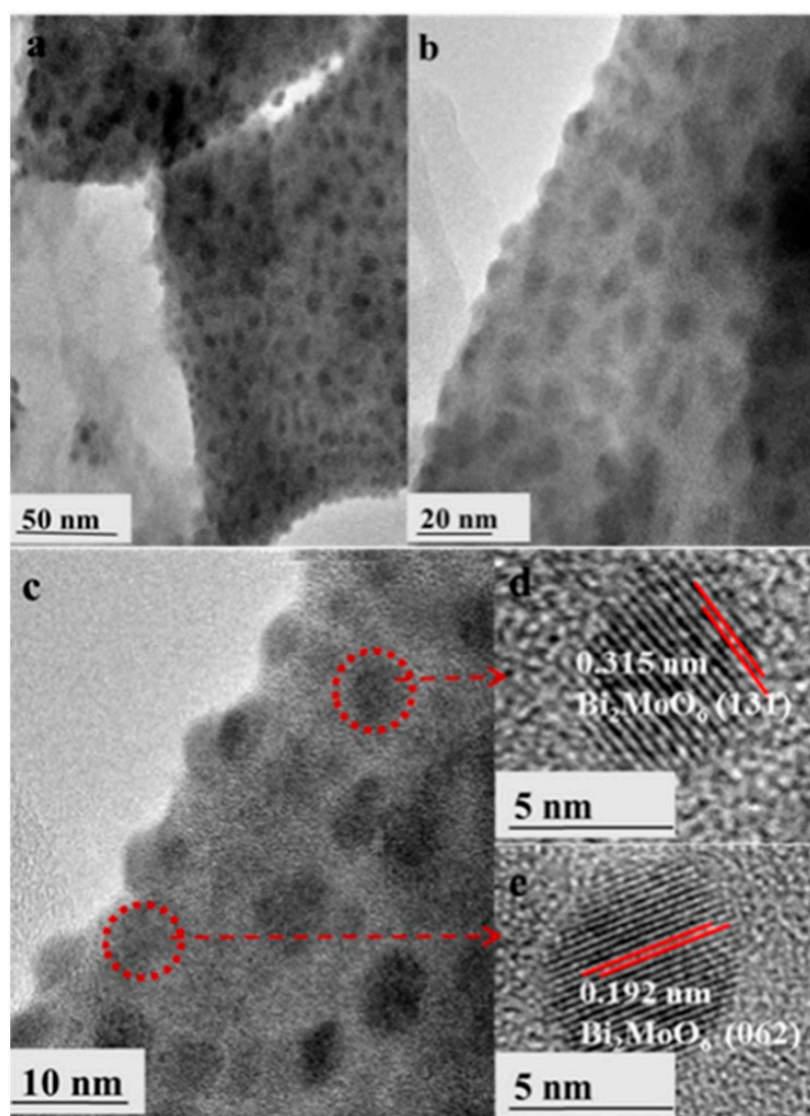


Figure 5. (a,b) TEM and (c–e) HRTEM images of Bi_2MoO_6 QD/ $\text{g-C}_3\text{N}_4$ nanocomposite [62]. Copyright 2019, Elsevier.

3.3. Other Metal Oxide QD- $\text{g-C}_3\text{N}_4$ Nanocomposites

Sun et al. sought to create CeO_2 quantum dots anchored on $\text{g-C}_3\text{N}_4$ ($\text{CeO}_2/\text{g-C}_3\text{N}_4$) and examine the photocatalytic performance of the material [63]. The creation of CeO_2 quantum dots anchored on $\text{g-C}_3\text{N}_4$ —which are anticipated to have improved photocatalytic properties—represents the work's originality (Figure 6). It is anticipated that the combination of these materials will enhance charge separation and increase the light absorption range. XRD, FTIR, SEM, TEM, XPS, and PL were used to characterize the synthesized $\text{CeO}_2/\text{g-C}_3\text{N}_4$. The outcomes demonstrated a homogeneous distribution of CeO_2 quantum dots on the $\text{g-C}_3\text{N}_4$ nanosheets. Better light absorption was discovered to be indicated with the bandgap of $\text{CeO}_2/\text{g-C}_3\text{N}_4$ being narrower than that of pure $\text{g-C}_3\text{N}_4$. By observing the degradation of Rhodamine B (RhB) under visible light irradiation, the photocatalytic performance was assessed. Compared to pure $\text{g-C}_3\text{N}_4$, the $\text{CeO}_2/\text{g-C}_3\text{N}_4$ demonstrated improved photocatalytic activity. The better charge separation and expanded light absorption range brought on with the presence of CeO_2 quantum dots are credited with the improved performance. Rhodamine B degradation under visible light showed higher photocatalytic performance from the $\text{CeO}_2/\text{g-C}_3\text{N}_4$ combination. This improved performance is a result of the cooperative action of $\text{g-C}_3\text{N}_4$ and CeO_2 quantum dots, which improves charge separa-

tion and light absorption. Although the exact findings section was not directly extracted, it may be deduced from the information given that the researchers were successful in creating CeO_2 quantum dots anchored on $\text{g-C}_3\text{N}_4$ with enhanced photocatalytic characteristics. Its improved Rhodamine B degradation under visible light made the composite material an attractive option for photocatalytic applications.

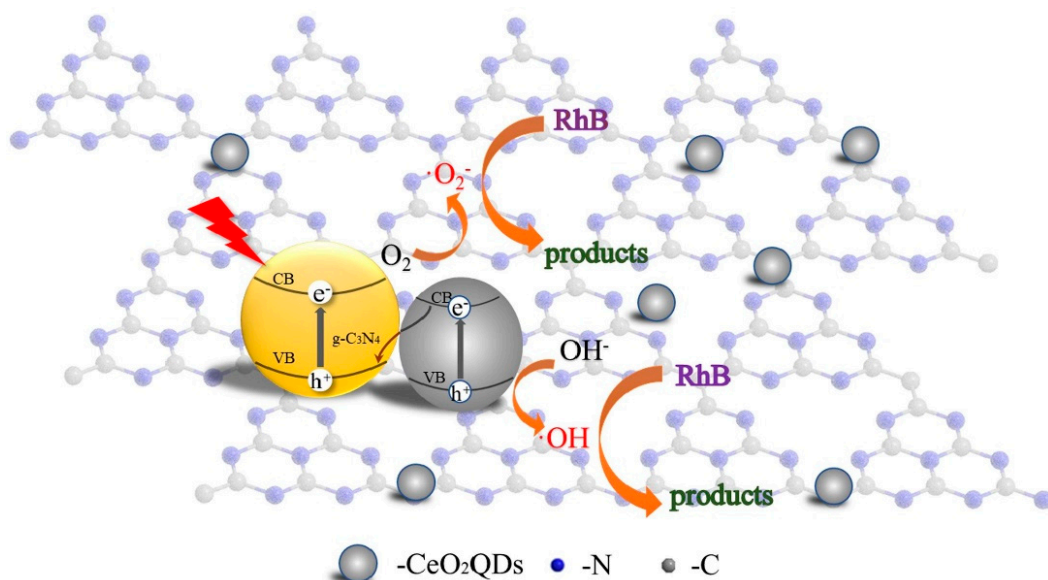


Figure 6. The photocatalytic RhB degradation mechanism over CeO_2 QD-modified $\text{g-C}_3\text{N}_4$ nanocomposite [63]. Copyright 2022, Elsevier.

In order to create a novel photocatalyst, Zhu et al. combined $\text{g-C}_3\text{N}_4$ nanosheets and MoO_3 quantum dots (QDs). This mixture was created with the goal of improving photocatalytic activity for the reduction in U(VI) under visible light. The addition of MoO_3 QDs to $\text{g-C}_3\text{N}_4$ nanosheets is what makes this work novel [19]. Following their easy hydrothermal synthesis, the MoO_3 QDs were loaded onto $\text{g-C}_3\text{N}_4$ nanosheets using a straightforward ultrasonic dispersion technique. This mixture was predicted to facilitate photogenerated electron–hole pair separation and improve photocatalytic activity. The MoO_3 QD/ $\text{g-C}_3\text{N}_4$ nanosheets showed remarkable photocatalytic performance for U(VI) reduction when exposed to visible light in their as-prepared state. It was discovered that MoO_3 QDs should be loaded at a rate of 2%. The efficient separation of photogenerated electron–hole pairs and the expanded light absorption range were credited with the improved photocatalytic activity. Various characterization approaches were used to support the postulated photocatalytic mechanism. By measuring the concentration of U(VI) in aqueous solutions while they were exposed to visible light, the photocatalytic performance was assessed. The outcomes demonstrated that the photocatalytic reduction rate for U(VI) was greater in the MoO_3 QD/ $\text{g-C}_3\text{N}_4$ nanosheets than in pure $\text{g-C}_3\text{N}_4$. It can be concluded that $\text{g-C}_3\text{N}_4$ nanosheets in combination with MoO_3 QDs present a viable method for improving the photocatalytic reduction in U(VI) under visible light. The proposed mechanism and the innovative photocatalyst design offer important new perspectives for this field's future study. The detailed description of recent research on the photocatalytic abilities of nanocomposites based on metal oxide QD's- $\text{g-C}_3\text{N}_4$ were provided in Table 1.

Table 1. Detailed description of recent research on the photocatalytic abilities of nanocomposites based on metal oxide QDs-g-C₃N₄.

Photocatalyst	Pollutant	Dosage	Light Source	Efficiency	Ref.
SnO ₂ QDs/g-C ₃ N ₄	RhB	50 mg/L	Visible light	95% in 60 min	[51]
TiO ₂ QDs/g-C ₃ N ₄	RhB	10 mg/L	Visible light	99% in 75 min	[44]
TiO ₂ QDs/g-C ₃ N ₄	Phenol	10 mg/L	Visible light	98% in 100 min	[44]
TiO ₂ QDs/g-C ₃ N ₄	Cr (VI)	20 mg/L	Visible light	99% in 60 min	[44]
TiO ₂ QDs/g-C ₃ N ₄	MO	10 mg/L	Solar light	98% in 120 min	[20]
CeO ₂ QDs/g-C ₃ N ₄	RhB	10 mg/L	Visible light	80% in 180 min	[63]
CeO ₂ QDs/g-C ₃ N ₄	MO	10 mg/L	Visible light	82% in 180 min	[63]
CeO ₂ QDs/g-C ₃ N ₄	MB	10 mg/L	Visible light	74% in 180 min	[63]
BiVO ₄ QDs-g-C ₃ N ₄	RhB	10 mg/L	Visible light	81% in 90 min	[59]
Bi ₂ O ₃ QDs/g-C ₃ N ₄	TC	10 mg/L	Visible light	83% in 120 min	[60]
Bi ₂ O ₃ QDs/g-C ₃ N ₄	Cr (VI)	10 mg/L	Visible light	88% in 60 min	[60]
Bi ₂ O ₄ QDs/g-C ₃ N ₄	RhB	10 mg/L	Visible light	78% in 160 min	[64]
Bi ₂ WO ₆ QDs/g-C ₃ N ₄	MBT	20 mg/L	Visible light	99% in 80 min	[61]
MoO ₃ QDs/g-C ₃ N ₄	U (VI)	50 mg/L	Visible light	96% in 150 min	[19]
Co ₃ O ₄ QDs-g-C ₃ N ₄	MTZ	10 mg/L	Visible light	77% in 180 min	[18]
Bi ₂ WO ₆ QDs/g-C ₃ N ₄	NO	0.5 ppm	Visible light	61%	[31]
SnO ₂ QDs/g-C ₃ N ₄	NO	600 ppb	Visible light	32%	[29]
SnO ₂ NPs/g-C ₃ N ₄	RhB	10 ppm	Visible light	97% in 50 min	[65]
SnO ₂ NPs/g-C ₃ N ₄	MB	10 ppm	Visible light	99% in 90 min	[66]
SnO ₂ NPs/g-C ₃ N ₄	CR	10 ppm	Visible light	96% in 90 min	[66]
SnO ₂ NPs/g-C ₃ N ₄	NO	500 ppb	Visible light	40%	[67]
SnO ₂ NPs/g-C ₃ N ₄	RhB	10 ppm	Solar light	86% in 240 min	[68]
TiO ₂ NPs/g-C ₃ N ₄	TC	20 ppm	Visible light	99% in 120 min	[69]
TiO ₂ NPs/g-C ₃ N ₄	TC	20 ppm	UV light	96% in 90 min	[70]
TiO ₂ NPs/g-C ₃ N ₄	TC	20 ppm	Visible light	90% in 120 min	[71]
TiO ₂ NPs/g-C ₃ N ₄	MB	20 ppm	Solar light	80% in 180 min	[72]
TiO ₂ NPs/g-C ₃ N ₄	TC	100 ppm	Visible light	80% in 100 min	[73]
ZnO NPs/g-C ₃ N ₄	MB	10 ppm	Visible light	98% in 150 min	[74]
ZnO NPs/g-C ₃ N ₄	MB	50 ppm	Visible light	98% in 180 min	[75]
ZnO NPs/g-C ₃ N ₄	MB	10 ppm	Visible light	60% in 120 min	[76]
ZnO NPs/g-C ₃ N ₄	MB	10 ppm	Visible light	92% in 120 min	[77]
ZnO NPs/g-C ₃ N ₄	CR	10 ppm	Visible light	70% in 45 min	[78]
CeO ₂ NPs/g-C ₃ N ₄	MO	10 ppm	Visible light	96% in 100 min	[79]
CeO ₂ NPs/g-C ₃ N ₄	RhB	10 ppm	Visible light	96% in 60 min	[80]
CeO ₂ NPs/g-C ₃ N ₄	Cr	20 ppm	Visible light	96% in 100 min	[81]
CeO ₂ QDs/g-C ₃ N ₄	TC	10 ppm	Visible light	78% in 160 min	[82]
CeO ₂ NPs/g-C ₃ N ₄	MB	10 ppm	Visible light	70% in 180 min	[83]
BiVO ₄ NPs/g-C ₃ N ₄	4-CP	20 ppm	Visible light	95% in 100 min	[84]
BiVO ₄ NPs/g-C ₃ N ₄	MO	20 ppm	Visible light	82% in 60 min	[85]
BiVO ₄ NPs/g-C ₃ N ₄	MB	10 ppm	Visible light	88% in 120 min	[86]
BiVO ₄ NPs/g-C ₃ N ₄	TC	10 ppm	Visible light	89% in 120 min	[86]
Bi ₂ WO ₆ NPs/g-C ₃ N ₄	CIP	15 ppm	Visible light	98% in 120 min	[87]
Bi ₂ WO ₆ NPs/g-C ₃ N ₄	Diuron	20 ppm	Visible light	75% in 120 min	[88]
Bi ₂ WO ₆ NPs/g-C ₃ N ₄	ADN	10 ppm	Visible light	98% in 80 min	[89]
Co ₃ O ₄ NPs/g-C ₃ N ₄	Atrazine	-	Visible light	78% in 35 min	[90]
MoO ₃ NPs/g-C ₃ N ₄	TC	10 ppm	Visible light	86% in 100 min	[91]
MoO ₃ NPs/g-C ₃ N ₄	RhB	10 ppm	Visible light	99% in 25 min	[92]

Zhao et al. set out to create phosphorus-doped g-C₃N₄/Co₃O₄ quantum dots in a single step using vitamin B12. They sought to increase the synthesized substance's visible-light photocatalytic activity for the destruction of metronidazole (MTZ) [18]. The innovative aspect of the process is the one-step production of phosphorus-doped g-C₃N₄/Co₃O₄ quantum dots using vitamin B12. This technique is distinctive because it enhances the photocatalytic performance of g-C₃N₄ by combining the traits of both phosphorus doping and Co₃O₄ quantum dots. Several approaches were used to characterize the synthesized composites. The photodegradation of MTZ under visible light irradiation was used to

assess the photocatalytic activities of the composites. The explanation for the increased photocatalytic activity was determined to be the synergistic interaction between the produced Co_3O_4 quantum dots and P-doped g-C₃N₄. This interaction improved photo-induced electron and hole separation efficiency, prevented their recombination, and reduced band gap energy. The generated Co_3O_4 quantum dots and P-doped g-C₃N₄ worked together to enhance the photocatalytic performance of the created material. As a result of this synergy, photoinduced electrons and holes were separated and transferred more effectively, which increased the photocatalytic degradation of MTZ. The study successfully demonstrated the synthesis of g-C₃N₄/Co₃O₄ quantum dots doped with phosphorus utilizing a one-step procedure and vitamin B12. The created substance demonstrated improved visible-light photocatalytic activity for the breakdown of MTZ. The fundamental causes of the enhanced photocatalytic performance were determined to be the synergistic interactions between the produced Co_3O_4 quantum dots and P-doped g-C₃N₄.

The heterojunctions formed between traditional QDs like CdS/CdSe and g-C₃N₄ have demonstrated effective charge separation due to their staggered band alignment, which minimizes recombination and enhances photocatalytic performance. We discussed how these strategies of interface engineering can be applied to metal oxide QDs to optimize their interactions with g-C₃N₄, focusing on creating synergistic band alignments that facilitate charge transfer and extend light absorption. In-depth analyses of the photocatalytic mechanisms in CdS/CdSe and Ag-In-Zn-S QDs combined with g-C₃N₄ have revealed critical factors such as quantum confinement effects, surface states, and the role of co-catalysts in improving photocatalytic activity. By integrating these insights, we will elaborate on how similar principles might govern the activity of metal oxide QDs, and how understanding these mechanisms can guide the optimization of their photocatalytic performance. Drawing parallels between the successes of these traditional QDs and our subject metal oxide QDs, we will discuss how strategies like precise size control, doping, or the introduction of defects, successful in traditional QDs, can be mirrored in metal oxides to modulate band structure, enhance light absorption, and improve charge carrier dynamics. While acknowledging the efficiency of traditional QDs, we also recognize concerns regarding their toxicity and environmental impact, particularly for Cd-based QDs. This contrast presents an opportunity to highlight the relative environmental friendliness of metal oxide QDs and the importance of pursuing these materials for sustainable photocatalysis.

Carbon quantum dots (CQDs) have emerged as a captivating class of carbon nanomaterials, characterized by their unique optical, electrical, and physicochemical properties. These properties, combined with their aqueous stability, low toxicity, high surface area, economic feasibility, and tunable photoluminescence behavior, make them promising candidates for photocatalytic applications. On the other hand, graphitic carbon nitride (g-C₃N₄) has gained attention as a stable carbon-based polymer with potential applications in various fields. The combination of CQDs and g-C₃N₄ offers a synergistic effect, enhancing the adsorptive and photocatalytic activity of the resulting nanocomposite. This is attributed to the broader visible-light absorption, increased specific surface area, and enhanced electron-hole pair migration and separation efficiency of the composite. Comparatively, while metal oxide quantum dots also present potential in photocatalytic applications, the CQDs and g-C₃N₄ combination stands out due to its non-toxic nature, economic feasibility, and enhanced photoluminescence properties. The interaction within this multicomponent photocatalyst promotes photocatalytic performance, making it a superior choice for wastewater treatment and other environmental applications. In essence, the amalgamation of CQDs and g-C₃N₄ presents a novel and efficient approach to address the challenges of wastewater treatment, emphasizing the importance of continued research in this domain [93].

4. Conclusions and Perspectives

Quantum dots (QDs) and graphitic carbon nitride (g-C₃N₄) together highlight a developing area of study with the potential to advance the photocatalytic frontier. Harnessing the unique electronic, optical, and photocatalytic properties intrinsic to QDs such as ZnO,

SnO_2 , TiO_2 , CeO_2 , CO_3O_4 , MoO_3 , BiVO_4 , Bi_2O_3 , Bi_2WO_6 , Bi_2O_4 , and Bi_2MoO_6 , when juxtaposed with the properties of $\text{g-C}_3\text{N}_4$, promises a synergy that could redefine the boundaries of photocatalysis. As we reflect on our discussions, let us draw some conclusions and speculate on future avenues.

Synergy of QDs with $\text{g-C}_3\text{N}_4$: quantum dots and $\text{g-C}_3\text{N}_4$ can be used to enhance light absorption, improve charge transfer, and reduce electron–hole recombination. This enhances their overall photocatalytic efficacy and paves the way for efficient light-driven reactions, particularly those aimed at energy conversion and environmental remediation.

Diverse Quantum Dot Landscape: each QD brings its unique characteristics. For instance, ZnO and TiO_2 QDs have been heralded for their UV light-driven photocatalytic activities, while the bismuth-based QDs such as BiVO_4 , Bi_2O_3 , and Bi_2WO_6 exhibit visible light-driven capabilities. The inherent bandgap variations, coupled with different photo-corrosion resistances and surface chemistries, provide a diverse landscape for tailoring the desired photocatalytic response.

Enhanced Stability and Sustainability: one of the perennial challenges with photocatalysts is their stability and recyclability. $\text{g-C}_3\text{N}_4$'s structural robustness, when combined with the protective attributes of QDs, leads to prolonged catalyst life, thereby elevating the potential for sustainable and scalable applications.

Heterostructuring and Multifunctionality: in addition to enhancing the activity of the quantum dots, the addition of $\text{g-C}_3\text{N}_4$ also brings multifunctionality. The heterostructures formed can serve as platforms for multiple simultaneous reactions, like water splitting alongside organic pollutant degradation, creating avenues for multifaceted photocatalytic systems.

5. Future Perspectives

Tailored Photocatalytic Systems: given the plethora of QDs available, future research should focus on systematically tailoring QD- $\text{g-C}_3\text{N}_4$ combinations to target specific photocatalytic reactions. This tailoring could lead to breakthroughs in reaction efficiency and selectivity.

Deep Dive into Charge Dynamics: to optimize the QD- $\text{g-C}_3\text{N}_4$ interfaces further, a comprehensive understanding of charge dynamics, including the rates of charge transfer, recombination, and trapping, is crucial. Advanced spectroscopic and microscopic techniques could elucidate these intricacies.

Scale-up and Real-world Applications: the transition from lab-scale research to real-world applications requires addressing challenges related to catalyst scale-up, stability under fluctuating environmental conditions, and integration with existing industrial setups.

Holistic Environmental Impact: as we push the boundaries of photocatalysis, it is imperative to ensure the green synthesis of these QD- $\text{g-C}_3\text{N}_4$ systems, minimizing any adverse environmental footprints and maximizing their eco-friendly applications.

Z-Schemes and Ternary Nanocomposites: researchers have the opportunity to explore and construct Z-scheme-based systems using QDs and $\text{g-C}_3\text{N}_4$. Additionally, there is potential for designing ternary nanocomposites, such as metal oxide QD- $\text{g-C}_3\text{N}_4$ -noble metals, metal oxide QD- $\text{g-C}_3\text{N}_4$ -carbon-related materials, and more.

In closing, the fusion of quantum dots with $\text{g-C}_3\text{N}_4$ heralds a new era in photocatalysis. The potential breakthroughs discussed here are just the tip of the iceberg. As research intensifies, the full spectrum of possibilities will undoubtedly be unveiled, driving a cleaner, greener, and energy-efficient future.

Author Contributions: Conceptualization, methodology, validation, writing—original draft preparation, T.T.S.; formal analysis, resources, data curation, writing—original draft preparation, T.R.G.; writing—review and editing, supervision, B.B.; supervision, project administration, funding acquisition, K.Y. All authors have read and agreed to the published version of the manuscript.

Funding: This work was supported with a National Research Foundation of Korea (NRF) grant funded by the Korean government (MSIT) (No. 2021R1C1C1011089).

Data Availability Statement: Not applicable.

Conflicts of Interest: The authors declare that they have no conflict of interest regarding the publication of this article, financial and/or otherwise.

References

- Opoku, E.E.O.; Boachie, M.K. The environmental impact of industrialization and foreign direct investment. *Energy Policy* **2020**, *137*, 111178. [[CrossRef](#)]
- Tran, V.V.; Park, D.; Lee, Y.-C. Indoor Air Pollution, Related Human Diseases, and Recent Trends in the Control and Improvement of Indoor Air Quality. *Int. J. Environ. Res. Public Health* **2020**, *17*, 2927. [[CrossRef](#)] [[PubMed](#)]
- Antoci, A.; Galeotti, M.; Sordi, S. Environmental pollution as engine of industrialization. *Commun. Nonlinear Sci. Numer. Simul.* **2018**, *58*, 262–273. [[CrossRef](#)]
- Siddiqua, A.; Hahladakis, J.N.; Al-Attiya, W.A.K.A. An overview of the environmental pollution and health effects associated with waste landfilling and open dumping. *Environ. Sci. Pollut. Res.* **2022**, *29*, 58514–58536. [[CrossRef](#)]
- Manisalidis, I.; Stavropoulou, E.; Stavropoulos, A.; Bezirtzoglou, E. Environmental and Health Impacts of Air Pollution: A Review. *Front. Public Health* **2020**, *8*, 14. [[CrossRef](#)]
- He, J.; Kumar, A.; Khan, M.; Lo, I.M.C. Critical review of photocatalytic disinfection of bacteria: From noble metals- and carbon nanomaterials-TiO₂ composites to challenges of water characteristics and strategic solutions. *Sci. Total Environ.* **2021**, *758*, 143953. [[CrossRef](#)]
- Wei, Z.; Liu, J.; Shangguan, W. A review on photocatalysis in antibiotic wastewater: Pollutant degradation and hydrogen production. *Chin. J. Catal.* **2020**, *41*, 1440–1450. [[CrossRef](#)]
- Zhang, F.; Wang, X.; Liu, H.; Liu, C.; Wan, Y.; Long, Y.; Cai, Z. Recent Advances and Applications of Semiconductor Photocatalytic Technology. *Appl. Sci.* **2019**, *9*, 2489. [[CrossRef](#)]
- Guo, Q.; Zhou, C.; Ma, Z.; Yang, X. Fundamentals of TiO₂ Photocatalysis: Concepts, Mechanisms, and Challenges. *Adv. Mater.* **2019**, *31*, 1901997. [[CrossRef](#)]
- Wang, J.; Guo, R.-T.; Bi, Z.-X.; Chen, X.; Hu, X.; Pan, W.-G. A review on TiO₂–x-based materials for photocatalytic CO₂ reduction. *Nanoscale* **2022**, *14*, 11512–11528. [[CrossRef](#)]
- Zhao, Y.; Zhang, S.; Shi, R.; Waterhouse, G.I.N.; Tang, J.; Zhang, T. Two-dimensional photocatalyst design: A critical review of recent experimental and computational advances. *Mater. Today* **2020**, *34*, 78–91. [[CrossRef](#)]
- Li, X.; Xiong, J.; Gao, X.; Huang, J.; Feng, Z.; Chen, Z.; Zhu, Y. Recent advances in 3D g-C₃N₄ composite photocatalysts for photocatalytic water splitting, degradation of pollutants and CO₂ reduction. *J. Alloys Compd.* **2019**, *802*, 196–209. [[CrossRef](#)]
- Luo, Y.; Zhu, Y.; Han, Y.; Ye, H.; Liu, R.; Lan, Y.; Xue, M.; Xie, X.; Yu, S.; Zhang, L.; et al. g-C₃N₄-based photocatalysts for organic pollutant removal: A critical review. *Carbon Res.* **2023**, *2*, 14. [[CrossRef](#)]
- Chen, L.; Maigbay, M.A.; Li, M.; Qiu, X. Synthesis and modification strategies of g-C₃N₄ nanosheets for photocatalytic applications. *Adv. Powder Mater.* **2023**, *100150*, *in press*. [[CrossRef](#)]
- Zhu, W.; Yue, Y.; Wang, H.; Zhang, B.; Hou, R.; Xiao, J.; Huang, X.; Ishag, A.; Sun, Y. Recent advances on energy and environmental application of graphitic carbon nitride (g-C₃N₄)-based photocatalysts: A review. *J. Environ. Chem. Eng.* **2023**, *11*, 110164. [[CrossRef](#)]
- Babu, B.; Koutavarapu, R.; Shim, J.; Yoo, K. Enhanced visible-light-driven photoelectrochemical and photocatalytic performance of Au-SnO₂ quantum dot-anchored g-C₃N₄ nanosheets. *Sep. Purif. Technol.* **2020**, *240*, 116652. [[CrossRef](#)]
- Jin, T.; Liu, C.B.; Chen, F.; Qian, J.C.; Qiu, Y.B.; Meng, X.R.; Chen, Z.G. Synthesis of g-C₃N₄/CQDs composite and its photocatalytic degradation property for Rhodamine B. *Carbon Lett.* **2022**, *32*, 1451–1462. [[CrossRef](#)]
- Zhao, Z.W.; Fan, J.Y.; Deng, X.Y.; Liu, J. One-step synthesis of phosphorus-doped g-C₃N₄/Co₃O₄ quantum dots from vitamin B12 with enhanced visible-light photocatalytic activity for metronidazole degradation. *Chem. Eng. J.* **2019**, *360*, 1517–1529. [[CrossRef](#)]
- Zhu, X.; Dong, Z.M.; Xu, J.D.; Lin, S.Y.; Liu, J.Y.; Cheng, Z.P.; Cao, X.H.; Wang, Y.Q.; Liu, Y.H.; Zhang, Z.B. Visible-light induced electron-transfer in MoO₃ QDs/g-C₃N₄ nanosheets for efficient photocatalytic reduction of U(VI). *J. Alloys Compd.* **2022**, *926*, 10. [[CrossRef](#)]
- Guo, R.T.; Liu, X.Y.; Qin, H.; Ang, Z.Y.; Shi, X.; Pan, W.G.; Fu, Z.G.; Tang, J.Y.; Jia, P.Y.; Miao, Y.F.; et al. Photocatalytic reduction of CO₂ into CO over nanostructure Bi₂S₃ quantum dots/g-C₃N₄ composites with Z-scheme mechanism. *Appl. Surf. Sci.* **2020**, *500*, 144059. [[CrossRef](#)]
- Wang, J.M.; Yu, L.M.; Wang, Z.J.; Wei, W.; Wang, K.F.; Wei, X.H. Constructing 0D/2D Z-Scheme Heterojunction of CdS/g-C₃N₄ with Enhanced Photocatalytic Activity for H-2 Evolution. *Catal. Lett.* **2021**, *151*, 3550–3561. [[CrossRef](#)]
- Li, G.; Huang, J.M.; Wang, N.N.; Huang, J.L.; Zheng, Y.M.; Zhan, G.W.; Li, Q.B. Carbon quantum dots functionalized g-C₃N₄ nanosheets as enhanced visible-light photocatalysts for water splitting. *Diam. Relat. Mat.* **2021**, *116*, 9. [[CrossRef](#)]
- Huo, Y.; Ding, X.H.; Zhang, X.Y.; Ren, M.; Sang, L.B.; Wen, S.Y.; Song, D.Y.; Yang, Y.X. Graphene quantum dot implanted supramolecular carbon nitrides with robust photocatalytic activity against recalcitrant contaminants. *Catal. Sci. Technol.* **2022**, *12*, 3937–3946. [[CrossRef](#)]

24. Hu, X.Y.; Yu, Y.T.; Chen, D.D.; Xu, W.C.; Fang, J.Z.; Liu, Z.; Li, R.Q.; Yao, L.; Qin, J.J.; Fang, Z.Q. Anatase/Rutile homojunction quantum dots anchored on g-C₃N₄ nanosheets for antibiotics degradation in seawater matrice via coupled adsorption-photocatalysis: Mechanism insight and toxicity evaluation. *Chem. Eng. J.* **2022**, *432*, 15. [[CrossRef](#)]
25. Zhao, T.Y.; Xing, Z.P.; Xiu, Z.Y.; Li, Z.Z.; Yang, S.L.; Zhou, W. Oxygen-Doped MoS₂ Nanospheres/CdS Quantum Dots/g-C₃N₄ Nanosheets Super-Architectures for Prolonged Charge Lifetime and Enhanced Visible-Light-Driven Photocatalytic Performance. *ACS Appl. Mater. Interfaces* **2019**, *11*, 7104–7111. [[CrossRef](#)]
26. Wu, H.H.; Yu, S.Y.; Wang, Y.; Han, J.; Wang, L.; Song, N.; Dong, H.J.; Li, C.M. A facile one-step strategy to construct 0D/2D SnO₂/g-C₃N₄ heterojunction photocatalyst for high-efficiency hydrogen production performance from water splitting. *Int. J. Hydrogen Energy* **2020**, *45*, 30142–30152. [[CrossRef](#)]
27. Babu, B.; Cho, M.; Byon, C.; Shim, J. Sunlight-driven photocatalytic activity of SnO₂ QDs-g-C₃N₄ nanolayers. *Mater. Lett.* **2018**, *212*, 327–331. [[CrossRef](#)]
28. Li, N.X.; Liu, X.C.; Zhou, J.C.; Chen, W.S.; Liu, M.C. Encapsulating CuO quantum dots in MIL-125(Ti) coupled with g-C₃N₄ for efficient photocatalytic CO₂ reduction. *Chem. Eng. J.* **2020**, *399*, 11. [[CrossRef](#)]
29. Zou, Y.Z.; Xie, Y.; Yu, S.; Chen, L.; Cui, W.; Dong, F.; Zhou, Y. SnO₂ quantum dots anchored on g-C₃N₄ for enhanced visible-light photocatalytic removal of NO and toxic NO₂ inhibition. *Appl. Surf. Sci.* **2019**, *496*, 8. [[CrossRef](#)]
30. Zhu, Z.; Tang, X.; Fan, W.Q.; Liu, Z.; Huo, P.W.; Wang, T.S.; Yan, Y.S.; Li, C.X. Studying of Co-doped g-C₃N₄ and modified with Fe₃O₄ quantum dots on removing tetracycline. *J. Alloys Compd.* **2019**, *775*, 248–258. [[CrossRef](#)]
31. Cheng, C.; Chen, D.Y.; Li, N.J.; Li, H.; Xu, Q.F.; He, J.H.; Lu, J.M. Bi₂WO₆ quantum dots with oxygen vacancies combined with g-C₃N₄ for NO removal. *J. Colloid Interface Sci.* **2022**, *609*, 447–455. [[CrossRef](#)] [[PubMed](#)]
32. Paul, D.R.; Sharma, R.; Nehra, S.P.; Sharma, A. Effect of calcination temperature, pH and catalyst loading on photodegradation efficiency of urea derived graphitic carbon nitride towards methylene blue dye solution. *RSC Adv.* **2019**, *9*, 15381–15391. [[CrossRef](#)] [[PubMed](#)]
33. Surender, S.; Balakumar, S. Insight into the melamine-derived freeze-dried nanostructured g-C₃N₄ for expeditious photocatalytic degradation of dye pollutants. *Diam. Relat. Mat.* **2022**, *128*, 109269. [[CrossRef](#)]
34. Raaja Rajeshwari, M.; Kokilavani, S.; Sudheer Khan, S. Recent developments in architecturing the g-C₃N₄ based nanostructured photocatalysts: Synthesis, modifications and applications in water treatment. *Chemosphere* **2022**, *291*, 132735. [[CrossRef](#)]
35. Fernández-Catalá, J.; Greco, R.; Navlani-García, M.; Cao, W.; Berenguer-Murcia, Á.; Cazorla-Amorós, D. g-C₃N₄-Based Direct Z-Scheme Photocatalysts for Environmental Applications. *Catalysts* **2022**, *12*, 1137. [[CrossRef](#)]
36. Hayat, A.; Sohail, M.; El Jery, A.; Al-Zaydi, K.M.; Alshammari, K.F.; Khan, J.; Ali, H.; Ajmal, Z.; Taha, T.A.; Ud Din, I.; et al. Different Dimensionalities, Morphological Advancements and Engineering of g-C₃N₄-Based Nanomaterials for Energy Conversion and Storage. *Chem. Rec.* **2023**, *23*, e202200171. [[CrossRef](#)]
37. Linh, P.H.; Do Chung, P.; Van Khien, N.; Oanh, L.T.M.; Thu, V.T.; Bach, T.N.; Hang, L.T.; Hung, N.M.; Lam, V.D. A simple approach for controlling the morphology of g-C₃N₄ nanosheets with enhanced photocatalytic properties. *Diam. Relat. Mat.* **2021**, *111*, 108214. [[CrossRef](#)]
38. Zhang, M.; Yang, Y.; An, X.; Zhao, J.; Bao, Y.; Hou, L.-A. Exfoliation method matters: The microstructure-dependent photoactivity of g-C₃N₄ nanosheets for water purification. *J. Hazard. Mater.* **2022**, *424*, 127424. [[CrossRef](#)]
39. Chen, Y.; Yang, B.; Xie, W.; Zhao, X.; Wang, Z.; Su, X.; Yang, C. Combined soft templating with thermal exfoliation toward synthesis of porous g-C₃N₄ nanosheets for improved photocatalytic hydrogen evolution. *J. Mater. Res. Technol.* **2021**, *13*, 301–310. [[CrossRef](#)]
40. Wu, X.; Gao, D.; Wang, P.; Yu, H.; Yu, J. NH₄Cl-induced low-temperature formation of nitrogen-rich g-C₃N₄ nanosheets with improved photocatalytic hydrogen evolution. *Carbon* **2019**, *153*, 757–766. [[CrossRef](#)]
41. Zhou, L.; Shen, Z.; Wang, S.; Gao, J.; Tang, L.; Li, J.; Dong, Y.; Wang, Z.; Lyu, J. Construction of quantum-scale catalytic regions on anatase TiO₂ nanoparticles by loading TiO₂ quantum dots for the photocatalytic degradation of VOCs. *Ceram. Int.* **2021**, *47*, 21090–21098. [[CrossRef](#)]
42. Javed, S.; Islam, M.; Mujahid, M. Synthesis and characterization of TiO₂ quantum dots by sol gel reflux condensation method. *Ceram. Int.* **2019**, *45*, 2676–2679. [[CrossRef](#)]
43. Wang, S.; Wang, F.; Su, Z.; Wang, X.; Han, Y.; Zhang, L.; Xiang, J.; Du, W.; Tang, N. Controllable Fabrication of Heterogeneous p-TiO₂ QDs@g-C₃N₄ p-n Junction for Efficient Photocatalysis. *Catalysts* **2019**, *9*, 439. [[CrossRef](#)]
44. Wang, J.; Lin, W.; Hu, H.; Liu, C.; Cai, Q.; Zhou, S.; Kong, Y. Engineering Z-system hybrids of 0D/2D F-TiO₂ quantum dots/g-C₃N₄ heterostructures through chemical bonds with enhanced visible-light photocatalytic performance. *New J. Chem.* **2021**, *45*, 3067–3078. [[CrossRef](#)]
45. Lee, J.-H.; Jeong, S.-Y.; Son, Y.-D.; Lee, S.-W. Facile Fabrication of TiO₂ Quantum Dots-Anchored g-C₃N₄ Nanosheets as 0D/2D Heterojunction Nanocomposite for Accelerating Solar-Driven Photocatalysis. *Nanomaterials* **2023**, *13*, 1565. [[CrossRef](#)]
46. Kumari, K.; Ahmaruzzaman, M. SnO₂ quantum dots (QDs): Synthesis and potential applications in energy storage and environmental remediation. *Mater. Res. Bull.* **2023**, *168*, 112446. [[CrossRef](#)]
47. Yu, B.; Li, Y.; Wang, Y.; Li, H.; Zhang, R. Facile hydrothermal synthesis of SnO₂ quantum dots with enhanced photocatalytic degradation activity: Role of surface modification with chloroacetic acid. *J. Environ. Chem. Eng.* **2021**, *9*, 105618. [[CrossRef](#)]
48. Xu, Z.; Jiang, Y.; Li, Z.; Chen, C.; Kong, X.; Chen, Y.; Zhou, G.; Liu, J.-M.; Kempa, K.; Gao, J. Rapid Microwave-Assisted Synthesis of SnO₂ Quantum Dots for Efficient Planar Perovskite Solar Cells. *ACS Appl. Energy Mater.* **2021**, *4*, 1887–1893. [[CrossRef](#)]

49. Bathula, B.; Gurugubelli, T.R.; Yoo, J.; Yoo, K. Recent Progress in the Use of SnO₂ Quantum Dots: From Synthesis to Photocatalytic Applications. *Catalysts* **2023**, *13*, 765. [[CrossRef](#)]
50. Wu, Z.; Jing, H.; Zhao, Y.; Lu, K.; Liu, B.; Yu, J.; Xia, X.; Lei, W.; Hao, Q. Grain boundary and interface interaction Co-regulation promotes SnO₂ quantum dots for efficient CO₂ reduction. *Chem. Eng. J.* **2023**, *451*, 138477. [[CrossRef](#)]
51. Yousaf, M.U.; Pervaiz, E.; Minallah, S.; Afzal, M.J.; Honghong, L.; Yang, M. Tin oxide quantum dots decorated graphitic carbon nitride for enhanced removal of organic components from water: Green process. *Results Phys.* **2019**, *14*, 102455. [[CrossRef](#)]
52. Ji, H.; Fan, Y.; Yan, J.; Xu, Y.; She, X.; Gu, J.; Fei, T.; Xu, H.; Li, H. Construction of SnO₂/graphene-like g-C₃N₄ with enhanced visible light photocatalytic activity. *RSC Adv.* **2017**, *7*, 36101–36111. [[CrossRef](#)]
53. Mohamed, K.M.; Benitto, J.J.; Vijaya, J.J.; Bououdina, M. Recent Advances in ZnO-Based Nanostructures for the Photocatalytic Degradation of Hazardous, Non-Biodegradable Medicines. *Crystals* **2023**, *13*, 329. [[CrossRef](#)]
54. Mohamed, W.A.A.; Handal, H.T.; Ibrahem, I.A.; Galal, H.R.; Mousa, H.A.; Labib, A.A. Recycling for solar photocatalytic activity of Dianix blue dye and real industrial wastewater treatment process by zinc oxide quantum dots synthesized by solvothermal method. *J. Hazard. Mater.* **2021**, *404*, 123962. [[CrossRef](#)]
55. Mohamed, W.A.A.; Ibrahem, I.A.; El-Sayed, A.M.; Galal, H.R.; Handal, H.; Mousa, H.A.; Labib, A.A. Zinc oxide quantum dots for textile dyes and real industrial wastewater treatment: Solar photocatalytic activity, photoluminescence properties and recycling process. *Adv. Powder Technol.* **2020**, *31*, 2555–2565. [[CrossRef](#)]
56. Ye, Q.; Xu, L.; Xia, Y.; Gang, R.; Xie, C. Zinc oxide quantum dots/graphitic carbon nitride nanosheets based visible-light photocatalyst for efficient tetracycline hydrochloride degradation. *J. Porous Mat.* **2022**, *29*, 571–581. [[CrossRef](#)]
57. Ren, Z.; Ma, H.; Geng, J.; Liu, C.; Song, C.; Lv, Y. ZnO QDs/GO/g-C₃N₄ Preparation and Photocatalytic Properties of Composites. *Micromachines* **2023**, *14*, 1501. [[CrossRef](#)]
58. Vattikuti, S.V.P.; Reddy, P.A.K.; Shim, J.; Byon, C. Visible-Light-Driven Photocatalytic Activity of SnO₂–ZnO Quantum Dots Anchored on g-C₃N₄ Nanosheets for Photocatalytic Pollutant Degradation and H₂ Production. *ACS Omega* **2018**, *3*, 7587–7602. [[CrossRef](#)]
59. Wang, J.B.; Liu, C.; Yang, S.; Lin, X.; Shi, W.L. Fabrication of a ternary heterostructure BiVO₄ quantum dots/C-60/g-C₃N₄ photocatalyst with enhanced photocatalytic activity. *J. Phys. Chem. Solids* **2020**, *136*, 7. [[CrossRef](#)]
60. Liang, Y.; Xu, W.; Fang, J.; Liu, Z.; Chen, D.; Pan, T.; Yu, Y.; Fang, Z. Highly dispersed bismuth oxide quantum dots/graphite carbon nitride nanosheets heterojunctions for visible light photocatalytic redox degradation of environmental pollutants. *Appl. Catal. B* **2021**, *295*, 120279. [[CrossRef](#)]
61. Zeng, Y.; Yin, Q.; Liu, Z.; Dong, H. Attapulgite-interpenetrated g-C₃N₄/Bi₂WO₆ quantum-dots Z-scheme heterojunction for 2-mercaptopbenzothiazole degradation with mechanism insight. *Chem. Eng. J.* **2022**, *435*, 134918. [[CrossRef](#)]
62. Ding, F.; Chen, P.; Liu, F.; Chen, L.; Guo, J.-K.; Shen, S.; Zhang, Q.; Meng, L.-H.; Au, C.-T.; Yin, S.-F. Bi₂MoO₆/g-C₃N₄ of 0D/2D heterostructure as efficient photocatalyst for selective oxidation of aromatic alkanes. *Appl. Surf. Sci.* **2019**, *490*, 102–108. [[CrossRef](#)]
63. Sun, Y.; Yuan, X.; Wang, Y.; Zhang, W.; Li, Y.; Zhang, Z.; Su, J.; Zhang, J.; Hu, S. CeO₂ quantum dots anchored g-C₃N₄: Synthesis, characterization and photocatalytic performance. *Appl. Surf. Sci.* **2022**, *576*, 151901. [[CrossRef](#)]
64. Qin, Y.Y.; Li, H.; Lu, J.; Ma, C.C.; Liu, X.L.; Meng, M.J.; Yan, Y.S. Fabrication of magnetic quantum dots modified Z-scheme Bi₂O₄/g-C₃N₄ photocatalysts with superior hydroxyl radical productivity for the degradation of rhodamine B. *Appl. Surf. Sci.* **2019**, *493*, 458–469. [[CrossRef](#)]
65. Sun, C.; Yang, J.; Zhu, Y.; Xu, M.; Cui, Y.; Liu, L.; Ren, W.; Zhao, H.; Liang, B. Synthesis of 0D SnO₂ nanoparticles/2D g-C₃N₄ nanosheets heterojunction: Improved charge transfer and separation for visible-light photocatalytic performance. *J. Alloys Compd.* **2021**, *871*, 159561. [[CrossRef](#)]
66. Mohammad, A.; Khan, M.E.; Karim, M.R.; Cho, M.H. Synergistically effective and highly visible light responsive SnO₂-g-C₃N₄ nanostructures for improved photocatalytic and photoelectrochemical performance. *Appl. Surf. Sci.* **2019**, *495*, 143432. [[CrossRef](#)]
67. Van Pham, V.; Mai, D.-Q.; Bui, D.-P.; Van Man, T.; Zhu, B.; Zhang, L.; Sangkaworn, J.; Tantirungrotechai, J.; Reutrakul, V.; Cao, T.M. Emerging 2D/0D g-C₃N₄/SnO₂ S-scheme photocatalyst: New generation architectural structure of heterojunctions toward visible-light-driven NO degradation. *Environ. Pollut.* **2021**, *286*, 117510. [[CrossRef](#)]
68. Wang, X.; He, Y.; Xu, L.; Xia, Y.; Gang, R. SnO₂ particles as efficient photocatalysts for organic dye degradation grown in-situ on g-C₃N₄ nanosheets by microwave-assisted hydrothermal method. *Mater. Sci. Semicond. Process.* **2021**, *121*, 105298. [[CrossRef](#)]
69. Zhang, B.; He, X.; Yu, C.; Liu, G.; Ma, D.; Cui, C.; Yan, Q.; Zhang, Y.; Zhang, G.; Ma, J.; et al. Degradation of tetracycline hydrochloride by ultrafine TiO₂ nanoparticles modified g-C₃N₄ heterojunction photocatalyst: Influencing factors, products and mechanism insight. *Chin. Chem. Lett.* **2022**, *33*, 1337–1342. [[CrossRef](#)]
70. Ni, S.; Fu, Z.; Li, L.; Ma, M.; Liu, Y. Step-scheme heterojunction g-C₃N₄/TiO₂ for efficient photocatalytic degradation of tetracycline hydrochloride under UV light. *Colloids Surf. A Physicochem. Eng. Asp.* **2022**, *649*, 129475. [[CrossRef](#)]
71. Guo, F.; Sun, H.; Huang, X.; Shi, W.; Yan, C. Fabrication of TiO₂/high-crystalline g-C₃N₄ composite with enhanced visible-light photocatalytic performance for tetracycline degradation. *J. Chem. Technol. Biotechnol.* **2020**, *95*, 2684–2693. [[CrossRef](#)]
72. Gündoğmuş, P.; Park, J.; Öztürk, A. Preparation and photocatalytic activity of g-C₃N₄/TiO₂ heterojunctions under solar light illumination. *Ceram. Int.* **2020**, *46*, 21431–21438. [[CrossRef](#)]
73. Li, Y.; Zhang, Q.; Lu, Y.; Song, Z.; Wang, C.; Li, D.; Tang, X.; Zhou, X. Surface hydroxylation of TiO₂/g-C₃N₄ photocatalyst for photo-Fenton degradation of tetracycline. *Ceram. Int.* **2022**, *48*, 1306–1313. [[CrossRef](#)]

74. Jung, H.; Pham, T.-T.; Shin, E.W. Effect of g-C₃N₄ precursors on the morphological structures of g-C₃N₄/ZnO composite photocatalysts. *J. Alloys Compd.* **2019**, *788*, 1084–1092. [[CrossRef](#)]
75. Ngullie, R.C.; Alaswad, S.O.; Bhuvaneswari, K.; Shanmugam, P.; Pazhanivel, T.; Arunachalam, P. Synthesis and Characterization of Efficient ZnO/g-C₃N₄ Nanocomposites Photocatalyst for Photocatalytic Degradation of Methylene Blue. *Coatings* **2020**, *10*, 500. [[CrossRef](#)]
76. Tan, X.; Wang, X.; Hang, H.; Zhang, D.; Zhang, N.; Xiao, Z.; Tao, H. Self-assembly method assisted synthesis of g-C₃N₄/ZnO heterostructure nanocomposites with enhanced photocatalytic performance. *Opt. Mater.* **2019**, *96*, 109266. [[CrossRef](#)]
77. Naseri, A.; Samadi, M.; Pourjavadi, A.; Ramakrishna, S.; Moshfegh, A.Z. Enhanced photocatalytic activity of ZnO/g-C₃N₄ nanofibers constituting carbonaceous species under simulated sunlight for organic dye removal. *Ceram. Int.* **2021**, *47*, 26185–26196. [[CrossRef](#)]
78. Mathialagan, A.; Manavalan, M.; Venkatachalam, K.; Mohammad, F.; Oh, W.C.; Sagadevan, S. Fabrication and physicochemical characterization of g-C₃N₄/ZnO composite with enhanced photocatalytic activity under visible light. *Opt. Mater.* **2020**, *100*, 109643. [[CrossRef](#)]
79. Xu, X.; Huang, T.; Xu, Y.; Hu, H.; Liao, S.; Hu, X.; Chen, D.; Zhang, M. Highly dispersed CeO_{2-x} nanoparticles with rich oxygen vacancies enhance photocatalytic performance of g-C₃N₄ toward methyl orange degradation under visible light irradiation. *J. Rare Earths* **2022**, *40*, 1255–1263. [[CrossRef](#)]
80. Subashini, A.; Varun Prasath, P.; Sagadevan, S.; Anita Lett, J.; Fatimah, I.; Mohammad, F.; Al-Lohedan, H.A.; Alshahateet, S.F.; Chun Oh, W. Enhanced photocatalytic degradation efficiency of graphitic carbon nitride-loaded CeO₂ nanoparticles. *Chem. Phys. Lett.* **2021**, *769*, 138441. [[CrossRef](#)]
81. Barathi, D.; Rajalakshmi, N.; Ranjith, R.; Sangeetha, R.; Meyvel, S. Controllable synthesis of CeO₂/g-C₃N₄ hybrid catalysts and its structural, optical and visible light photocatalytic activity. *Diam. Relat. Mat.* **2021**, *111*, 108161. [[CrossRef](#)]
82. Kaur, M.; Singh, S.; Mehta, S.K.; Kansal, S.K.; Umar, A.; Ibrahim, A.A.; Baskoutas, S. CeO₂ quantum dots decorated g-C₃N₄ nanosheets: A potential scaffold for fluorescence sensing of heavy metals and visible-light driven photocatalyst. *J. Alloys Compd.* **2023**, *960*, 170637. [[CrossRef](#)]
83. Wei, X.; Wang, X.; Pu, Y.; Liu, A.; Chen, C.; Zou, W.; Zheng, Y.; Huang, J.; Zhang, Y.; Yang, Y.; et al. Facile ball-milling synthesis of CeO₂/g-C₃N₄ Z-scheme heterojunction for synergistic adsorption and photodegradation of methylene blue: Characteristics, kinetics, models, and mechanisms. *Chem. Eng. J.* **2021**, *420*, 127719. [[CrossRef](#)]
84. Rathi, V.; Panneerselvam, A.; Sathiyapriya, R. A novel hydrothermal induced BiVO₄/g-C₃N₄ heterojunctions visible-light photocatalyst for effective elimination of aqueous organic pollutants. *Vacuum* **2020**, *180*, 109458. [[CrossRef](#)]
85. Xu, X.; Zhang, J.; Tao, F.; Dong, Y.; Wang, L.; Hong, T. Facile construction of Z-scheme g-C₃N₄/BiVO₄ heterojunctions for boosting visible-light photocatalytic activity. *Mater. Sci. Eng. B* **2022**, *279*, 115676. [[CrossRef](#)]
86. Reddy, C.V.; Nagar, A.; Shetti, N.P.; Reddy, I.N.; Basu, S.; Shim, J.; Kakarla, R.R. Novel g-C₃N₄/BiVO₄ heterostructured nanohybrids for high efficiency photocatalytic degradation of toxic chemical pollutants. *Chemosphere* **2023**, *322*, 138146. [[CrossRef](#)] [[PubMed](#)]
87. Mao, J.; Hong, B.; Wei, J.; Xu, J.; Han, Y.; Jin, H.; Jin, D.; Peng, X.; Li, J.; Yang, Y.; et al. Enhanced Ciprofloxacin Photodegradation of Visible-Light-Driven Z-Scheme g-C₃N₄/Bi₂WO₆ Nanocomposites and Interface Effect. *ChemistrySelect* **2019**, *4*, 13716–13723. [[CrossRef](#)]
88. Yasmeen, H.; Zada, A.; Li, W.; Xu, M.; Liu, S. Suitable energy platform of Bi₂WO₆ significantly improves visible-light degradation activity of g-C₃N₄ for highly toxic diuron pollutant. *Mater. Sci. Semicond. Process.* **2019**, *102*, 104598. [[CrossRef](#)]
89. Lian, X.; Xue, W.; Dong, S.; Liu, E.; Li, H.; Xu, K. Construction of S-scheme Bi₂WO₆/g-C₃N₄ heterostructure nanosheets with enhanced visible-light photocatalytic degradation for ammonium dinitramide. *J. Hazard. Mater.* **2021**, *412*, 125217. [[CrossRef](#)]
90. Yang, Q.; An, J.; Xu, Z.; Liang, S.; Wang, H. Performance and mechanism of atrazine degradation using Co₃O₄/g-C₃N₄ hybrid photocatalyst with peroxymonosulfate under visible light irradiation. *Colloids Surf. A Physicochem. Eng. Asp.* **2021**, *614*, 126161. [[CrossRef](#)]
91. Liu, L.; Huang, J.; Yu, H.; Wan, J.; Liu, L.; Yi, K.; Zhang, W.; Zhang, C. Construction of MoO₃ nanoparticles/g-C₃N₄ nanosheets 0D/2D heterojunction photocatalysts for enhanced photocatalytic degradation of antibiotic pollutant. *Chemosphere* **2021**, *282*, 131049. [[CrossRef](#)] [[PubMed](#)]
92. Xue, S.; Wu, C.; Pu, S.; Hou, Y.; Tong, T.; Yang, G.; Qin, Z.; Wang, Z.; Bao, J. Direct Z-Scheme charge transfer in heterostructured MoO₃/g-C₃N₄ photocatalysts and the generation of active radicals in photocatalytic dye degradations. *Environ. Pollut.* **2019**, *250*, 338–345. [[CrossRef](#)] [[PubMed](#)]
93. Liu, Y.; Huang, H.; Cao, W.; Mao, B.; Liu, Y.; Kang, Z. Advances in carbon dots: From the perspective of traditional quantum dots. *Mat. Chem. Front.* **2020**, *4*, 1586–1613. [[CrossRef](#)]

Disclaimer/Publisher's Note: The statements, opinions and data contained in all publications are solely those of the individual author(s) and contributor(s) and not of MDPI and/or the editor(s). MDPI and/or the editor(s) disclaim responsibility for any injury to people or property resulting from any ideas, methods, instructions or products referred to in the content.